A new mechanism-based temperature-dependent viscoelastic model for unidirectional polymer matrix composites based on Cartan decomposition

L. Di Gennaro, F. Daghia, M. Olive, Frédéric Jacquemin, D. Espinassou

A new mechanism-based thermo-viscoelastic model for unidirectional polymer matrix composites based on Cartan decomposition

L. Di Gennaro[a,*], F. Daghia[a], M. Olive[a], F. Jacquemin[b], D. Espinassou[c]

[a] *Université Paris-Saclay, ENS Paris-Saclay, CNRS, LMT - Laboratoire de Mécanique et Technologie, 4 avenue des Sciences, 91190, Gif-sur-Yvette, France.*
[b] *Institut de Recherche en Génie Civil et Mécanique (GeM) – UMR CNRS 6183, 58 Rue Michel Ange, 44600 Saint Nazaire, France*
[c] *CETIM, Technocampus Composites Chemin du Chaffault, 44340 Bouguenais, France*

Abstract

A new three-dimensional thermo-viscoelastic constitutive model for unidirectional fiber reinforced, polymer composite materials is developed in this work. The key point is to introduce the viscoelastic behavior only where appropriate, based on the constitutive behavior of the underlying constituents, elastic fibers and viscoelastic (in shear) matrix. In order to achieve this, an irreducible Cartan decomposition for the stress and strain tensors under the hypothesis of transverse isotropy is derived. The integrity basis for the decomposition is used to formulate the energy functional, which enables us to define uncoupled constitutive laws in which the contributions of the underlying constituents are easily identified. In order to describe the viscoelastic behavior in shear of the matrix, a generalized Maxwell model is applied to the appropriate terms of the stress and strain decomposition, in agreement with the underlying physical mechanism. Thermal strains and temperature effects on the viscoelastic behavior are introduced through the time-temperature superposition principle. Various numerical simulations are performed to show

*Corresponding author

Email addresses: livio.di_gennaro@ens-paris-saclay.fr (L. Di Gennaro), federica.daghia@ens-paris-saclay.fr (F. Daghia), marc.olive@ens-paris-saclay.fr (M. Olive), frederic.jacquemin@univ-nantes.fr (F. Jacquemin), Denis.Espinassou@cetim.fr (D. Espinassou)

the key features of the presented constitutive model and an Abaqus UMAT is implemented in order to perform structural simulations.

Keywords: Composite materials, Transversely isotropic, Cartan decomposition, Viscoelastic, Numerical methods, Residual stresses

---

1. Introduction

In the last decades, the use of composite materials has grown a lot, increasingly involving application which require high production rates, such as in the automotive industry. The introduction of modern and automated production techniques, like Laser Assisted Tape Placement (LATP), becomes crucial in this context, and it needs to be accompanied by the development of models which can predict the complex initial state induced in a composite structure by the manufacturing process. In particular, localized laser heating induces high temperature gradients in the structure, which require to account for the viscoelastic, temperature dependent behavior of the composite in order to achieve an accurate prediction of residual stresses and strains.

The Laser Assisted Tape Placement makes use of pre-impregnated tapes, containing long, oriented fibers embedded in a thermoplastic matrix: the basic building block of LATP structures is therefore a unidirectional fiber reinforced composite material. In particular, the fibers can be considered elastic and sustain most of the load, while the matrix shows a viscoelastic behavior in shear [1, 2]. Therefore, the mechanical properties are strongly direction dependent and, based on the material symmetries, a transversely isotropic behavior can be postulated. The aim of this paper is to develop an original constitutive model for a viscoelastic, temperature dependent composite, in which the viscoelastic behavior of the composite is defined based on the underlying physical mechanism described before, that is the viscoelastic shear response of the matrix.

For isotropic material models, the viscoelastic relaxation is generally described with a set of scalar parameters, each associated to a different relaxation time (see for example [3]). For anisotropic material models, on the other hand, different relaxation functions (or a relaxation tensor) are introduced to describe the viscoelastic behavior associated to each material parameter, without a clear link to the underlying physical mechanisms (as in [4, 5, 6]). It should be noted that, in the last reference [6], the transversely isotropic

elastic behavior is derived from an energy function based on invariants of the strain tensor.

A recent work which makes a clearer link between the viscoelastic behavior of the matrix and that of the resulting composite is the paper by Nedjar [7]. Starting from an energy-derived transversely isotropic elastic behavior based on invariants of the strain tensor, a particular stress/strain decomposition is introduced, following [8], and the viscoelastic behavior is only attributed to the terms of this decomposition related to the shear behavior of the matrix. A similar approach, although with some crucial differences, is adopted in this paper.

The key element of the present work, discussed in Section 2, consists in defining an irreducible decomposition [9] for the second order stress/strain tensors *before* defining the strain energy. An integrity basis for the energy function [10] can then been extracted, yielding naturally uncoupled constitutive equations for each element of the decomposition. Thanks to this rigorous mathematical formulation, the contributions of two underlying constituents of the composite material (fibers and matrix) to each term of the constitutive behavior become easy to identify. A generalized Maxwell model can then be applied only to the appropriate terms of the stress/strain decomposition in order to describe the viscoelastic behavior of the composite in agreement with the underlying physical mechanism, as discussed in Section 3.

In order to account for the evolution of the viscoelastic behavior with temperature, the thermal strains and the time-temperature superposition principle are introduced in Section 4, under the hypothesis of thermorheologically simple materials [11].

In Section 5, several numerical simulations are shown to highlight the key characteristics of the presented model. In particular, it is illustrated how the relaxation function associated to the transverse modulus of the composite is not an independent function, but it is related to the relaxation of the shear modulus in the plane of transverse isotropy. A user-material (UMAT) for the commercial finite element software Abaqus is developed in order to perform numerical simulations on structural parts.

Finally, in Section 6 conclusions and perspectives are discussed. The stress and strain tensors decomposition proposed in the present work enable us to address, in a relatively simple way, other physical mechanism related to each constituent, such as the crystallization kinetics in the matrix.

2. Transversely isotropic elastic behavior based on Cartan decomposition

The key point of the proposed model consists in defining the transversely isotropic elastic behavior of a unidirectional composite ply in terms of elementary, uncoupled material parameters, which can be physically related to the material parameters of the two underlying constituents, the fibers and the matrix. As it is discussed in the following, these uncoupled parameters do not exactly correspond to the classically defined elastic constants E_L, E_T, μ_L, μ_T and ν_{LT}.

The key to the definition of such an uncoupled behavior is to derive the elastic fourth order tensor from a quadratic energy function, formulated in terms of an appropriate minimal integrity basis [10]. Such an integrity basis, in turn, is defined by finding an irreducible O(2) decomposition [9] of the second order stress (and strain) tensor, where O(2) is the orthogonal group of the Euclidean plane, modeling the anisotropy.

The idea to use group representation theory [12] and make an irreducible decomposition of the second order stress or strain tensor has already been used in the case of the cubic anisotropy [13, 14, 15, 16, 17]. Furthermore, finding an explicit O(2) integrity basis can be straightforward using the recent publication [18], while some work was done in [19] about O(2) irreducible decomposition of strain tensor.

This rigorous mathematical formulation turns out to have deep physical significance, as it is discussed in the following. In particular, it enables us to clearly separate the material parameters which are influenced by the shear behavior of the matrix and, as such, which should display a viscoelastic long term behavior, from those which should remain elastic throughout the analysis. This approach is radically different from the one adopted in many viscoelastic models for transversely isotropic materials [4, 6, 5], which introduce different viscous relaxation functions for each of the classical elastic constants (E_L, E_T, μ_L, μ_T and ν_{LT}), with no clear link to the mechanical behavior of the underlying constituents. A similar, although not irreducible, decomposition of the stress (and strain) tensor, was proposed by [8] and used to model the viscoelastic response of unidirectional plies by [7], but only partial uncoupling is achieved in that case.

Let us introduce the fibers' direction vector $\boldsymbol{v}_f$, defining the normal to the isotropic plane $(\boldsymbol{v}_2, \boldsymbol{v}_3)$. The transverse isotropy is then modelled on the group generated by the rotations of axis $\boldsymbol{v}_f$, as well as the change of direction

of $\boldsymbol{v}_f$ (equivalently the rotation of axis $\boldsymbol{v}_2$ and angle π). Such a group is in fact the group O(2) of orthogonal transformation of the plane $(\boldsymbol{v}_2, \boldsymbol{v}_3)$. An O(2) irreducible decomposition of the stress tensor, also known as a Cartan decomposition [9], is for instance given as follows:

$$\boldsymbol{\sigma} = s_f \boldsymbol{M}_f + s_h \boldsymbol{M}_h + \boldsymbol{s}_{fs} + \boldsymbol{s}_d, \tag{1}$$

where

$$\begin{aligned} \boldsymbol{s}_{fs} &= s_{f2} \boldsymbol{M}_{f2} + s_{f3} \boldsymbol{M}_{f3}, \\ \boldsymbol{s}_d &= s_d \boldsymbol{M}_d + s_{23} \boldsymbol{M}_{23}, \end{aligned} \tag{2}$$

and the (unit) second order tensors $\boldsymbol{M}_\bullet$ are defined as

$$\begin{aligned} \boldsymbol{M}_f &= \boldsymbol{v}_f \otimes \boldsymbol{v}_f, \\ \boldsymbol{M}_h &= \frac{1}{\sqrt{2}} \left(\boldsymbol{v}_2 \otimes \boldsymbol{v}_2 + \boldsymbol{v}_3 \otimes \boldsymbol{v}_3 \right), \\ \boldsymbol{M}_{f2} &= \frac{1}{\sqrt{2}} \left(\boldsymbol{v}_f \otimes \boldsymbol{v}_2 + \boldsymbol{v}_2 \otimes \boldsymbol{v}_f \right), \\ \boldsymbol{M}_{f3} &= \frac{1}{\sqrt{2}} \left(\boldsymbol{v}_f \otimes \boldsymbol{v}_3 + \boldsymbol{v}_3 \otimes \boldsymbol{v}_f \right), \\ \boldsymbol{M}_d &= \frac{1}{\sqrt{2}} \left(\boldsymbol{v}_2 \otimes \boldsymbol{v}_2 - \boldsymbol{v}_3 \otimes \boldsymbol{v}_3 \right), \\ \boldsymbol{M}_{23} &= \frac{1}{\sqrt{2}} \left(\boldsymbol{v}_2 \otimes \boldsymbol{v}_3 + \boldsymbol{v}_3 \otimes \boldsymbol{v}_2 \right). \end{aligned} \tag{3}$$

It can be verified that the elements defined in the decomposition Eq. (1) are stable, that is they remain in the same space when subjected to operations belonging to the group. Indeed, we have for a rotation of axis $\boldsymbol{v}_f$ and angle θ:

$$\begin{aligned} &s_f \boldsymbol{M}_f + s_h \boldsymbol{M}_h \mapsto s_f \boldsymbol{M}_f + s_h \boldsymbol{M}_h \\ &s_{f2} \boldsymbol{M}_{f2} + s_{f3} \boldsymbol{M}_{f3} \mapsto (\cos(\theta) s_{f2} - \sin(\theta) s_{f3}) \boldsymbol{M}_{f2} + (\sin(\theta) s_{f2} + \cos(\theta) s_{f3}) \boldsymbol{M}_{f3} \\ &s_d \boldsymbol{M}_d + s_{23} \boldsymbol{M}_{23} \mapsto (\cos(2\theta) s_d - \sin(2\theta) s_{23}) \boldsymbol{M}_d + (\sin(2\theta) s_d + \cos(2\theta) s_{23}) \boldsymbol{M}_{23} \end{aligned} \tag{4}$$

Such a decomposition of the stress tensor is far from being unique. Indeed, any invertible linear combination

$$(\boldsymbol{M}_f, \boldsymbol{M}_h) \mapsto \alpha \boldsymbol{M}_f + \beta \boldsymbol{M}_h \tag{5}$$

leads to another Cartan decomposition of $\boldsymbol{\sigma}$. The specific decomposition chosen here is related to the physical interpretation of the obtained components, which is quite straightforward. Two of the four terms involve the $\boldsymbol{v}_f$ direction, namely s_f (normal stress in the fibers' direction) and $\boldsymbol{s}_{fs}$ (longitudinal shear stresses s_{fi}). The other two, s_h and $\boldsymbol{s}_d$, involve only the plane of transverse isotropy, and they are analogous to the classical hydrostatic/deviatoric decomposition in two dimensions. Since the tensors $\boldsymbol{M}_\bullet$ are orthogonal and of unit length by construction, each term $s_\bullet$ of the decomposition can be extracted from the complete tensor $\boldsymbol{\sigma}$ as $s_\bullet = \boldsymbol{\sigma} : \boldsymbol{M}_\bullet$.

From a direct application of [18], an O(2) integrity basis of $\boldsymbol{\sigma}$ is given by the 6 polynomials

$$I_1 := s_f, \quad J_1 := s_h, \quad I_2 := \|\boldsymbol{s}_{fs}\|^2, \quad J_2 := \|\boldsymbol{s}_d\|^2, \quad I_3 := \operatorname{tr}\left(\boldsymbol{s}_{fs}^2 \boldsymbol{s}_d\right), \quad (6)$$

meaning that any O(2) polynomial invariant I can be written as $I = p(I_1, J_1, I_2, J_2, I_3)$, with some polynomial p (see [10] for more details on integrity bases). The Gibbs free energy leading to linear elasticity can thus be defined using the 5 polynomial invariants

$$I_1^2 = s_f^2, \quad I_1 J_1 = s_f s_h, \quad J_1^2 = s_h^2, \quad I_2 = \|\boldsymbol{s}_{fs}\|^2, \quad J_2 = \|\boldsymbol{s}_d\|^2, \quad (7)$$

so it can be written as:

$$\bar{w} = \frac{1}{2} S_F s_f^2 + S_{FH} s_f s_h + \frac{1}{2} S_H s_h^2 + \frac{1}{2\mu_L} ||\boldsymbol{s}_{fs}||^2 + \frac{1}{2\mu_T} ||\boldsymbol{s}_d||^2,$$

where S_F, S_{FH}, S_H, μ_L and μ_T are the five elementary material parameters which define the transversely isotropic elastic behavior.

Knowing the Gibbs free energy, the strain can be then computed as:

$$\begin{aligned} \boldsymbol{\varepsilon} = \frac{\partial \bar{w}}{\partial \boldsymbol{\sigma}} &= \left(S_F s_f + S_{FH} s_h\right) \boldsymbol{M}_f + \left(S_{FH} s_f + S_H s_h\right) \boldsymbol{M}_h + \frac{1}{2\mu_L} \boldsymbol{s}_{fs} + \frac{1}{2\mu_T} \boldsymbol{s}_d \\ &= e_f \boldsymbol{M}_f + e_h \boldsymbol{M}_h + \boldsymbol{e}_{fs} + \boldsymbol{e}_d. \end{aligned} \quad (8)$$

As expected, the strain can also be set in terms of the Cartan decomposition.

The constitutive relations can finally be written as

$$\begin{aligned} \begin{bmatrix} e_f \\ e_h \end{bmatrix} &= \begin{bmatrix} S_F & S_{FH} \\ S_{FH} & S_H \end{bmatrix} \begin{bmatrix} s_f \\ s_h \end{bmatrix}, \\ \boldsymbol{e}_{fs} &= \frac{\boldsymbol{s}_{fs}}{2\mu_L}, \\ \boldsymbol{e}_d &= \frac{\boldsymbol{s}_d}{2\mu_T}. \end{aligned} \quad (9)$$

The first of Eq. (9) involves the normal stresses/strains in the fibers' direction (s_f/e_f), as well as the hydrostatic part of the stresses/strains in the plane of transverse anisotropy (s_h/e_h). These terms are coupled by the material constant S_{FH}; while a different linear combination of s_f and s_h could be chosen to further uncouple these terms, this is beyond the scope of this work. Physically, this part of the constitutive behavior is controlled by the fibers' elastic modulus, E_F, as well as by the bulk modulus of the polymer matrix, K_M. As E_F and K_M are generally considered elastic, the material constants S_F, S_{FH} and S_H are assumed as purely elastic in the following.

The second and third of Eq. (9) involve the longitudinal and transverse shear responses of the composite. These two parts of the composite's response are influenced by the shear modulus of the polymer matrix, μ_M. As the polymer is generally assumed to be viscoelastic in shear, a viscoelastic model is introduced for μ_L and μ_T in Section 3. In principle, the viscoelastic behavior of the matrix could have different effects on the longitudinal and transverse shear behaviors of the composite, thus two different viscoelastic relaxation functions could be considered, to be identified via computational homogenization or via direct experimental testing on the composite. This will be the subject of further work.

If the full compliance tensor $\boldsymbol{S}$, defined as $\boldsymbol{\varepsilon} = \boldsymbol{S} : \boldsymbol{\sigma}$, is needed (such as for the implementation of a user material in a standard finite element code), it can be written as

$$\begin{aligned}\boldsymbol{S} =& S_F \boldsymbol{M}_f \otimes \boldsymbol{M}_f + S_H \boldsymbol{M}_h \otimes \boldsymbol{M}_h + S_{FH} \left(\boldsymbol{M}_f \otimes \boldsymbol{M}_h + \boldsymbol{M}_h \otimes \boldsymbol{M}_f\right) \\ &+ \frac{1}{2\mu_L} \left(\boldsymbol{M}_{f2} \otimes \boldsymbol{M}_{f2} + \boldsymbol{M}_{f3} \otimes \boldsymbol{M}_{f3}\right) + \frac{1}{2\mu_T} \left(\boldsymbol{M}_d \otimes \boldsymbol{M}_d + \boldsymbol{M}_{23} \otimes \boldsymbol{M}_{23}\right).\end{aligned} \tag{10}$$

In practice, the inverse (stiffness) relations will be used in the implementation, but the compliance relations were derived here because of their easier physical interpretation.

Remarks.

- The parameters μ_L and μ_T are the classical longitudinal and transverse shear moduli of the composite ply. In order to identify the values of S_F, S_{FH} and S_H in terms of the classical material constants (E_L, E_T, μ_L, μ_T, ν_{LT}), one can choose the particular case $\boldsymbol{v}_f^{\mathrm{T}} = [1, 0, 0]$, $\boldsymbol{v}_2^{\mathrm{T}} = [0, 1, 0]$,

$\boldsymbol{v}_3^{\mathrm{T}} = [0, 0, 1]$. The compliance tensor $\boldsymbol{S}$ yields

$$\boldsymbol{S} = \begin{pmatrix} S_F & \frac{S_{FH}}{\sqrt{2}} & \frac{S_{FH}}{\sqrt{2}} & 0 & 0 & 0 \\ \frac{S_{FH}}{\sqrt{2}} & \frac{S_H}{2} + \frac{1}{4\mu_T} & \frac{S_H}{2} - \frac{1}{4\mu_T} & 0 & 0 & 0 \\ \frac{S_{FH}}{\sqrt{2}} & \frac{S_H}{2} - \frac{1}{4\mu_T} & \frac{S_H}{2} + \frac{1}{4\mu_T} & 0 & 0 & 0 \\ 0 & 0 & 0 & \frac{1}{2\mu_T} & 0 & 0 \\ 0 & 0 & 0 & 0 & \frac{1}{2\mu_L} & 0 \\ 0 & 0 & 0 & 0 & 0 & \frac{1}{2\mu_L} \end{pmatrix}. \tag{11}$$

This can be compared to the classical compliance tensor written in the material basis

$$\boldsymbol{S} = \begin{pmatrix} \frac{1}{\mathrm{E}_L} & -\frac{\nu_{LT}}{\mathrm{E}_L} & -\frac{\nu_{LT}}{\mathrm{E}_L} & 0 & 0 & 0 \\ -\frac{\nu_{LT}}{\mathrm{E}_L} & \frac{1}{\mathrm{E}_T} & -\frac{\nu_{TT}}{\mathrm{E}_T} & 0 & 0 & 0 \\ -\frac{\nu_{LT}}{\mathrm{E}_L} & -\frac{\nu_{TT}}{\mathrm{E}_T} & \frac{1}{\mathrm{E}_T} & 0 & 0 & 0 \\ 0 & 0 & 0 & \frac{1}{2\mu_T} & 0 & 0 \\ 0 & 0 & 0 & 0 & \frac{1}{2\mu_L} & 0 \\ 0 & 0 & 0 & 0 & 0 & \frac{1}{2\mu_L} \end{pmatrix}, \tag{12}$$

leading to the following identification, from the terms (1,1), (1,2) and (2,2)

$$\begin{aligned} S_F &= \frac{1}{E_L}, \\ S_{FH} &= -\frac{\sqrt{2}\nu_{LT}}{E_L}, \\ S_H &= \frac{2}{E_T} - \frac{1}{2\mu_T}. \end{aligned} \tag{13}$$

It should be noticed that, since S_H is assumed as purely elastic in the following, the viscous relaxation of the transverse modulus E_T is directly related to the viscous relaxation of the transverse shear modulus μ_T, and not an independent function of time.

Finally, the fourth equation, term (2,3), yields the well-known transverse isotropy condition:

$$\mu_T = \frac{E_T}{2\left(1 + \nu_{TT}\right)}. \tag{14}$$

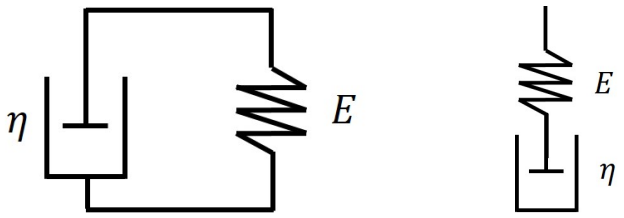

Figure 1: Basic rhelogical units: Kelvin-Voigt (left) and Maxwell (right)

- The decomposition proposed in Eq. (1) is similar to the one introduced in [8] and used by [7] to model the viscoelastic response of unidirectional plies. The decomposition proposed in those works, however, is derived *a posteriori* from internal constraints, and not defined *a priori* in a rigorous mathematical fashion as it is the case here. As a result, the material behavior obtained by [8, 7] is not fully uncoupled, and it is not possible to clearly separate the material parameters which are affected, or not, by the viscoelastic relaxation. This is the reason why the present approach was proposed here instead.

3. Linear viscoelasticity

A linear viscoelastic model is defined here and applied to the terms μ_L and μ_T of the behavior introduced in the previous Section.

Several viscoelastic models that can be found in the literature can be effectively understood by looking at their rheological representations. Combinations of springs and dash-pots can accurately represent and describe the material viscoelastic behavior.

The Kelvin-Voigt basic rheological unit is characterized by a spring and a dash-pot in parallel (Figure 1, left) and its one dimensional differential equation is:

$$s = Ee + \eta\dot{e}, \tag{15}$$

where E is the spring stiffness and η is the viscosity of the dash-pot. The generalized Kelvin-Voigt model, obtained by setting N different Kelvin-Voigt units (plus, eventually, a single spring) in series, is typically used to describe the material creep at constant stress.

The Maxwell basic rheological unit, on the other hand, is characterized by a spring and a dash-pot in series (Figure 1, right) and its one dimensional

differential equation is:

$$\frac{s}{\eta} + \frac{\dot{s}}{E} = \dot{e}. \tag{16}$$

The generalized Maxwell model (Figure 2), obtained by setting N different Maxwell units and a single spring in parallel, is typically used to characterize the stress relaxation at constant strain of the material. In particular, the characteristic relaxation time for a given Maxwell unit is $\tau = \frac{\eta}{E}$.

In the present case, a general loading path is sought, in which stress and strain both vary to satisfy the problem equations. In this case, both generalized Kelvin-Voigt and generalized Maxwell models can be successfully applied.

In the following, a generalized Maxwell model is considered for ease of implementation in a finite element setting. Indeed, in a classical finite element implementation, the search direction to determine stress and strain fields which satisfy the local constitutive behavior is taken at constant displacement. For this reason, the algorithms which solve the local constitutive equations are strain-driven, and each element of the generalized Maxwell model can be solved independently. Furthermore, based on the Boltzmann superposition principle, the model is formulated in integral form, which enables us to make use of well known literature results to achieve a simple and accurate numerical integration scheme.

The hereditary integrals for $\boldsymbol{s}_{fs}$ and $\boldsymbol{s}_d$ of the generalized Maxwell model are:

$$\begin{aligned} \boldsymbol{s}_{fs}(t) &= \int_0^t \Gamma_{fs}(t-t') \frac{d\boldsymbol{e}_{fs}(t')}{dt'} dt', \\ \boldsymbol{s}_d(t) &= \int_0^t \Gamma_d(t-t') \frac{d\boldsymbol{e}_d(t')}{dt'} dt', \end{aligned} \tag{17}$$

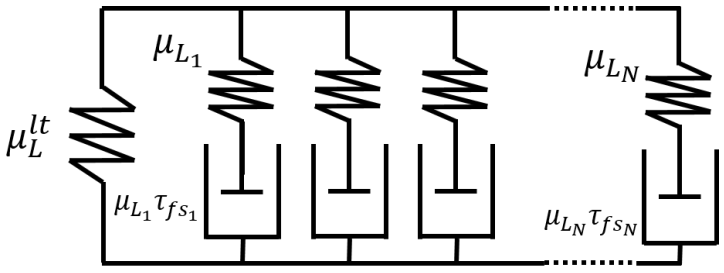

Figure 2: Material parameters for the Generalized Maxwell rheological model

where the relaxation functions Γ_{fs} and Γ_d, derived from solving Eq. (16) for each of the N Maxwell elements, can be written as follows:

$$\Gamma_{fs}(t-t') = 2\mu_L^{lt} + \sum_{j=1}^{N} 2\mu_{L_j} \exp\left(-\frac{t-t'}{\tau_{fs_j}}\right),$$
$$\Gamma_d(t-t') = 2\mu_T^{lt} + \sum_{j=1}^{N} 2\mu_{T_j} \exp\left(-\frac{t-t'}{\tau_{d_j}}\right). \tag{18}$$

In these expressions, the parameter μ_L^{lt} (resp. μ_T^{lt}) is associated to the isolated spring, and it represents the long term behavior once all stress relaxation has taken place. The parameter μ_{L_j} (resp. μ_{T_j}) is associated to the j-th spring, while τ_{fs_j} (resp. τ_{d_j}) is the relaxation time associated to the j-th Maxwell element.

From now on, only the mathematical development of the viscoelastic model for the terms $\boldsymbol{s}_{fs}$ and $\boldsymbol{e}_{fs}$ is detailed, as the two equations are identical in all except the material parameters. Substituting (18) into (17), it is possible to split the integral into a long term elastic part and a viscoelastic one:

$$\boldsymbol{s}_{fs}(t) = 2\mu_L^{lt}\boldsymbol{e}_{fs} + \sum_{j=1}^{N} \int_0^t 2\mu_{L_j} \exp\left(-\frac{t-t'}{\tau_{fs_j}}\right) \frac{d\boldsymbol{e}_{fs}(t')}{dt'} dt'. \tag{19}$$

Finally, from (19) $\boldsymbol{s}_{fs}$ can be decomposed as:

$$\boldsymbol{s}_{fs} = \boldsymbol{s}_{fs_0} + \sum_{j=1}^{N} \boldsymbol{g}_{fs_j}. \tag{20}$$

Eq. (20) shows how $\boldsymbol{s}_{fs}$ is obtained as a summation of an elastic stress $\left(\boldsymbol{s}_{fs_0} = 2\mu_L^{lt}\boldsymbol{e}_{fs}\right)$, and j internal viscoelastic stress variables $\boldsymbol{g}_{fs_j}$.

Finding an accurate and efficient numerical solution of the integral in Eq. (19) is crucial. Considering the time step $\Delta t = t^{n+1} - t^n$, and noting with a superscript i the quantities at time t^i, the elastic stress is readily computed as $\boldsymbol{s}_{fs_0}^{n+1} = 2\mu_L^{lt}\boldsymbol{e}_{fs}^{n+1}$, while the internal variables can be written as:

$$\boldsymbol{g}_{fs_j}^{n+1} = 2\mu_{L_j} \int_0^{t^{n+1}} \exp\left(-\frac{t^{n+1}-t'}{\tau_{fs_j}}\right) \frac{d\boldsymbol{e}_{fs}(t')}{dt'} dt'. \tag{21}$$

Remembering the properties of the integral and of the exponential function, we obtain:

$$\boldsymbol{g}_{fs_j}^{n+1} = \exp\left(-\frac{\Delta t}{\tau_{fs_j}}\right)\boldsymbol{g}_{fs_j}^{n} + 2\mu_{L_j}\int_{t_n}^{t_{n+1}} \exp\left(-\frac{t^{n+1}-t'}{\tau_{fs_j}}\right)\frac{d\boldsymbol{e}_{fs}(t')}{dt'}dt'. \quad (22)$$

This recursive formulation, first introduced in [20], is particularly efficient for large finite element problems, as it enables us to compute the internal variables at the current time instant t^{n+1}, knowing the information at the previous time instant t^n only, without needing to store the whole history of the material.

The finite difference approximation of the first derivative of the strain tensor $\boldsymbol{e}_{fs}$ enables us to compute the increment of the internal variables:

$$\frac{d\boldsymbol{e}_{fs}(t')}{dt'} \approx \frac{\boldsymbol{e}_{fs}^{n+1} - \boldsymbol{e}_{fs}^{n}}{\Delta t}. \quad (23)$$

Applying (23) to (22) we have:

$$\boldsymbol{g}_{fs_j}^{n+1} = \exp\left(-\frac{\Delta t}{\tau_{fs_j}}\right)\boldsymbol{g}_{fs_j}^{n} + 2\mu_{L_j}\int_{t_n}^{t_{n+1}} \exp\left(-\frac{t^{n+1}-t'}{\tau_{fs_j}}\right)dt'\left(\frac{\boldsymbol{e}_{fs}^{n+1} - \boldsymbol{e}_{fs}^{n}}{\Delta t}\right). \quad (24)$$

Solving the integral analytically, we finally obtain the following closed-form expression:

$$\boldsymbol{g}_{fs_j}^{n+1} = \exp\left(\frac{\Delta t}{\tau_{fs_j}}\right)\boldsymbol{g}_{fs_j}^{n} + \frac{1-\exp\left(\frac{\Delta t}{\tau_{fs_j}}\right)}{\left(\frac{\Delta t}{\tau_{fs_j}}\right)}2\mu_{L_j}\left[\boldsymbol{e}_{fs}^{n+1} - \boldsymbol{e}_{fs}^{n}\right]. \quad (25)$$

With analogous reasoning, the consistent tangent stiffness can be obtained as:

$$2\mu_L^{n+1} = \frac{\partial \boldsymbol{s}_{fs}^{n+1}}{\partial \boldsymbol{e}_{fs}^{n+1}} = 2\mu_L^{lt} + \sum_{j=1}^{N} 2\mu_{L_j}\frac{1-\exp\left(\frac{\Delta t}{\tau_{fs_j}}\right)}{\left(\frac{\Delta t}{\tau_{fs_j}}\right)}. \quad (26)$$

The full tangent constitutive tensor, useful to achieve efficient numerical solutions in commercial finite element codes, can be simply obtained by replacing the tangent values of μ_L and μ_T in Eq. (10).

Small values of $\left(\frac{\Delta t}{\tau_{fs_j}}\right)$ lead to cancellation error of the second term on the right-hand side of Eq. (25) and (26). In order to avoid this inconvenience, under these conditions the aforementioned term can be replaced by its Taylor series development as follows [21]:

$$\frac{1-\exp\left(\frac{\Delta t}{\tau_{fs_j}}\right)}{\left(\frac{\Delta t}{\tau_{fs_j}}\right)} \approx 1 - \frac{1}{2}\left(\frac{\Delta t}{\tau_{fs_j}}\right) + \frac{1}{6}\left(\frac{\Delta t}{\tau_{fs_j}}\right)^2. \tag{27}$$

It is important to notice that the only approximation introduced in the numerical solution is in Eq. (23), while the integral has been solved analytically. The resulting numerical integration algorithm is particularly accurate, even for large time increments.

Remarks. The parameters to be identified for the viscoelastic portion of the model are μ_L^{lt} (resp. μ_T^{lt}), as well as μ_{L_j} and τ_{fs_j} (resp. μ_{T_j} and τ_{d_j}) for each Maxwell element. In particular, μ_L^{lt}, related to $\boldsymbol{s}_{fs_0}$, is the long term modulus, once viscoelastic relaxation has completely occurred (that is, once the internal variables $\boldsymbol{g}_{fs_j}$ are null), while the short term (instantaneous) modulus is given by $\mu_L^{st} = \mu_L^{lt} + \sum_{j=1}^{N} \mu_{L_j}$. Experimental characterization at temperatures much lower than the reference temperature yield a measure of μ_L^{st}, while higher temperature tests over time scales similar to the relaxation time enable to evaluate the other viscoelastic properties.

4. Effects of temperature: thermal strains and time-temperature superposition

The viscoelastic response of the matrix and, consequently, of the composite, plays a crucial role in the establishment of residual stresses and strains during manufacturing processes involving high temperature gradients. In order to model these phenomena, temperature effects are included in the present model: in particular, the thermal strain is introduced, as well as the effect of temperature on viscoelasticity through time-temperature superposition.

In Section 2 the stress and strain Cartan decomposition was presented. The thermal strain can be decomposed in the same way to yield

$$\boldsymbol{\varepsilon}^{th} = e_f^{th}\boldsymbol{M}_f + e_h^{th}\boldsymbol{M}_h, \tag{28}$$

where

$$e_f^{th} = \alpha_1 \Delta T, \;\; e_h^{th} = \sqrt{2}\alpha_2 \Delta T, \tag{29}$$

and α_1 and α_2 are the coefficient thermal expansions in the fibers' direction and in the transverses directions, respectively. Therefore, the viscoelastic strain tensor can be written as:

$$\boldsymbol{\varepsilon}^{ve} = \left(e_f - e_f^{th}\right) \boldsymbol{M}_f + \left(e_h - e_h^{th}\right) \boldsymbol{M}_h + \boldsymbol{e}_{fs} + \boldsymbol{e}_d. \tag{30}$$

It is interesting to notice that the thermal strain does not contain the shear-related terms $\boldsymbol{e}_{fs}$ and $\boldsymbol{e}_d$, while the viscoelastic model presented in Section 3 only applies to these two terms. Consequently, any possible relaxation of the stresses induced by incompatible thermal strains cannot occur directly through the f and h portions of the behavior, which is purely elastic, but needs to be linked to the viscoelastic shear portions fs and d. Obviously, the link between the different portions of the behavior occurs through the directions of the stress and strain tensors imposed by the rest of the problem equations. This consideration, which is valid as well for classical isotropic thermo-visco-elastic behavior, is resumed in the rheological scheme of Fig. 3.

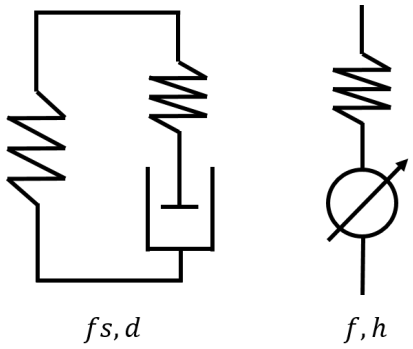

Figure 3: Rheological representation of the different portions of the composite's constitutive behavior: generalized Maxwell model to describe the viscoelastic shear portions (left) and the elastic portions with thermal strains (right)

The definition of the stress relaxation as a function of the temperature involves, for thermorheologically simple materials, the introduction of a new time scale called reduced time, which is a function of the temperature [11]. The reduced time is defined as follows:

$$t_{red} = \int_0^t \frac{1}{a(T)} dt'. \tag{31}$$

The shift function ($a(T)$) used here is the Williams-Landel-Ferry equation (WLF law):

$$\log\left[a(T)\right] = -\frac{C_1\left(T - T_{ref}\right)}{C_2 + \left(T - T_{ref}\right)}, \tag{32}$$

where T is the temperature, T_{ref} is the reference temperature for the polymer (generally coincident with the glass transition temperature) and C_1, C_2 are two material constants. The reduced time is used instead of the real time in the viscoelastic model equations of Section 3.

Depending on the composite's temperature, two extreme scenarios can occur (Fig. 4):

- for temperatures well above the reference temperature, the reduced time is much longer than the real time (and than the relaxation time), so stresses relaxation occurs nearly instantaneously,
- for temperatures much lower than the reference temperature, the reduced time is much shorter than the relaxation time, so the polymer is characterized by an elastic behavior in the time scale of interest.

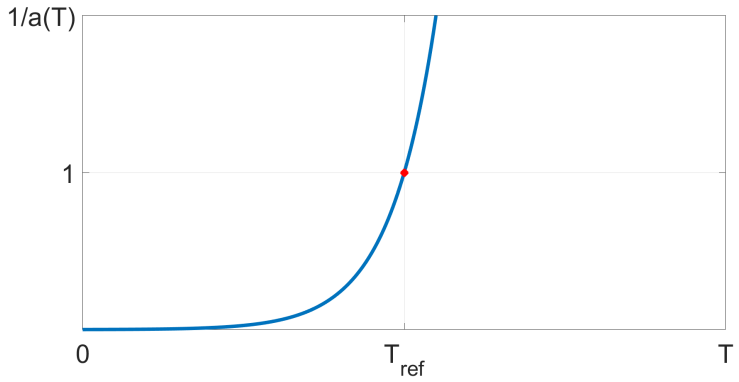

Figure 4: Reduced time as a function of temperature

Numerical integration of the reduced time is not trivial to compute over a non isothermal time step. Indeed, the shift function $a(T)$ is extremely nonlinear with the temperature. An approximation of the shift function could lead to large errors, therefore $h(T) = -\ln(a(T))$ is approximated instead, as a linear function of the temperature over the time increment [22]. Further

assuming the temperature T is a linear function of the time t over the time increment, follows:

$$h(T) = -\ln(a(T(t))) = A + Bt, \tag{33}$$

where the coefficients are readily obtained as

$$\begin{aligned} A &= \frac{t^{n+1}h(T^n) - t^n h(T^{n+1})}{\Delta t}, \\ B &= \frac{h(T^{n+1}) - h(T^n)}{\Delta t}. \end{aligned} \tag{34}$$

Therefore, from Eq. (31) the reduced time increment can be computed as follows:

$$\Delta t_{red} = \int_{t^n}^{t^{n+1}} \exp\left(A + Bt\right) dt, \tag{35}$$

which yields:

$$\Delta t_{red} = \frac{a^{-1}(T^{n+1}) - a^{-1}(T^n)}{h(T^{n+1}) - h(T^n)}. \tag{36}$$

5. Numerical simulations

In order to illustrate the main features of the proposed model, several numerical simulations are presented.

In Section 5.1, different loading histories are applied to a single material point in order to illustrate the model response in stress relaxation, creep and variable temperature tests. A Matlab implementation of the model is used for these examples.

In Section 5.2, on the other hand, the model is used within a thermo-mechanical structural simulation, in order to predict the residual stresses distributions within a composite structure for different surface cooling rates. The example is taken from [23], although in that case a different mechanical model was considered. An Abaqus UMAT was implemented to this end, using C language code generated from the original Matlab implementation via the Matlab Coder toolbox.

The instantaneous elastic parameters used for all simulations are the following [24]:

$$E_L = 134 \text{ GPa}, \quad E_T = 10.3 \text{ GPa}, \quad \mu_L = 6 \text{ GPa}, \quad \nu_{LT} = 0.32, \quad \nu_{TT} = 0.4.$$

Only one Maxwell element has been used for simplicity. The viscoelastic parameters are specified for each simulation.

5.1. Loading histories on a single material point

5.1.1. Stress relaxation tests

In order to simulate stress relaxation tests, a strain was imposed rapidly, then maintained until complete relaxation of the viscous term. Imposing different combinations of strain components, while setting the other stress components to zero, enables us to highlight some of the model features. Here, the fiber orientation vector was taken as $\boldsymbol{v}_f^{\mathrm{T}} = [1, 0, 0]$, thus the transverse isotropy direction is aligned with the x direction. For the simulations shown in this part, the viscoelastic parameters are taken as:

$$\mu_L^{lt} = 0.1\mu_L^{st}, \quad \mu_T^{lt} = 0.1\mu_T^{st}, \quad \tau_{fs} = 10 \text{ s}, \quad \tau_d = 10 \text{ s}.$$

The result obtained by imposing a shear strain $\varepsilon_{xy} = 0.005$ is depicted in Fig.(5). The evolution of the stress directly mirrors the evolution of the shear modulus μ_L as defined in Eq. (18).

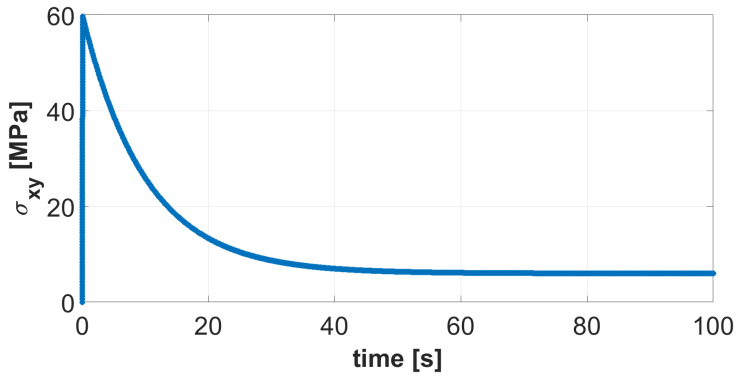

Figure 5: Shear stress relaxation for a constant imposed shear strain ($\varepsilon_{xy} = 0.005$)

Imposing a strain $\varepsilon_{yy} = 0.01$ in the transverse direction, on the other hand, enables us to observe the evolution of the transverse modulus E_T with time (see Figure 6). While other transversely isotropic material models, as [4, 6, 5], choose to specify different relaxation function for each of the five material parameters, here the relaxation of E_T is directly related to the relaxation of μ_T, as it can be noticed in the model equations. In particular, the short and long term values of E_T can be easily assessed as:

$$E_T = \frac{4\mu_T}{1 + 2\mu_T S_H}, \tag{37}$$

where S_H is constant and μ_T takes its short term and long term values, respectively. This is a distinguishing and very important feature of the proposed model.

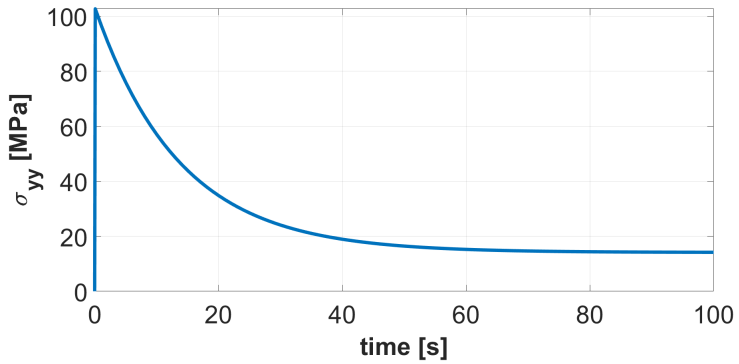

Figure 6: Transverse stress relaxation for a constant imposed transverse strain ($\varepsilon_{yy} = 0.01$)

More complex combinations of strains enable us to highlight the interplay between the different elements of the stress and strain decomposition. Imposing $\varepsilon_{yy} = 0.01$ and $\varepsilon_{zz} = 0$, the terms e_h and e_d are both constant and equal, and the stress response is the sum of the corresponding s_h and s_d terms. This is illustrated in Fig.(7).

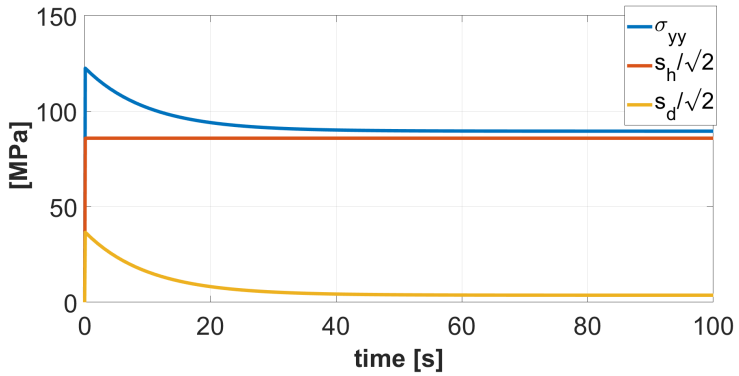

Figure 7: Transverse stress relaxation for a biaxial constant imposed strain state ($\varepsilon_{yy} = 0.01$, $\varepsilon_{zz} = 0$)

The e_h contribution can be easily turned off imposing $\varepsilon_{yy} = 0.01$ and $\varepsilon_{zz} = -0.01$. In this case, the stress relaxation is directly given by the evolution of μ_T (see Fig. (8)).

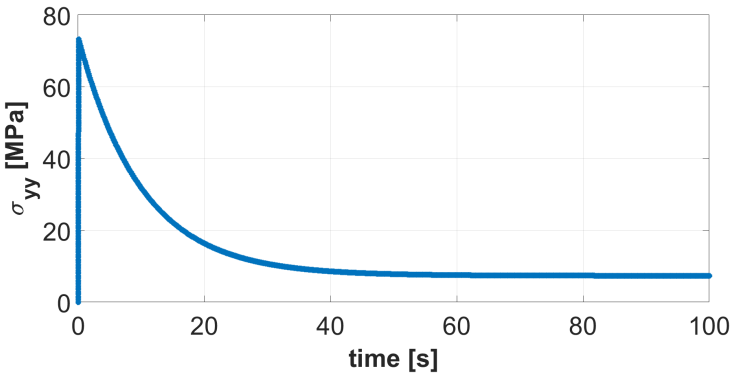

Figure 8: Transverse stress relaxation for a biaxial constant imposed strain state ($\varepsilon_{yy} = 0.01$, $\varepsilon_{zz} = -0.01$)

5.1.2. Creep tests

In this example, the effect of introducing different viscoelastic parameters for μ_L and μ_T is discussed using a creep test. Indeed, the viscoelastic behavior of the matrix could translate into different relaxation functions for μ_L and μ_T. Differently from [7], the model proposed here enables one to account for this effect. An investigation on this matter, based on the homogenization of a fiber/matrix representative volume element, is among the perspectives of this work.

In order to highlight the effect of each set of viscoelastic parameters, a constant stress $\sigma_{xx} = 100$ MPa was imposed, while the fiber direction $\boldsymbol{v}_f$ was rotated at different angles θ with respect to x.

Two different sets of simulations are depicted in Fig. (9). In the first, the viscoelastic parameters are

$$\mu_L^{lt} = 0.5\mu_L^{st}, \quad \mu_T^{lt} = 0.5\mu_T^{st}, \quad \tau_{fs} = 100 \text{ s}, \quad \tau_d = 100 \text{ s},$$

while, in the second, more relaxation is assumed to occur in the μ_T term:

$$\mu_L^{lt} = 0.5\mu_L^{st}, \quad \mu_T^{lt} = 0.28\mu_T^{st}, \quad \tau_{fs} = 100 \text{ s}, \quad \tau_d = 100 \text{ s}.$$

The difference between the two sets of parameters can be noticed, especially in the tests with large angles between the fibers and the loading direction. Indeed, in these transverse dominated directions, the term μ_T plays a more significant role, while μ_L is dominant for small angles. All viscoelastic contribution disappears completely for a load along the fibers's direction, which yields a purely elastic response.

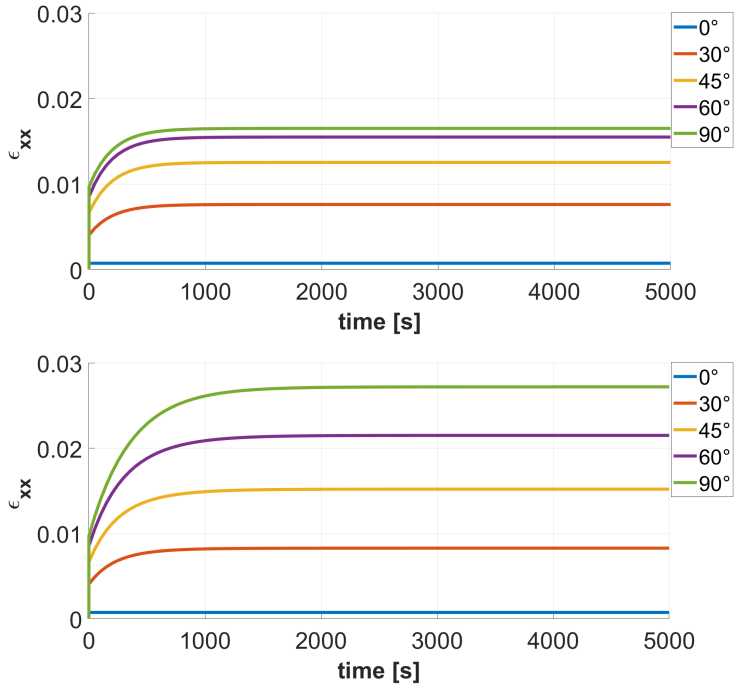

Figure 9: Creep loading tests for different angles θ between the loading and the fibers' direction, with the same relaxation functions (top) and with different relaxation functions (bottom) for μ_L and μ_T

5.1.3. Variable temperature tests

In order to see the effect of the temperature on stress relaxation, two simulations of a thermoplastic matrix composite cooling down from above its fusion point were carried out. A simple linear temperature function (to simulate a constant cooling rate from 400°C to 100°C in a time frame of 100 s) was used as input, and different restraints were imposed on the material point in order to evaluate their effect on the generation of thermal residual stresses. In this Section, the following viscoelastic parameters were used, to simulate the possibility of nearly complete relaxation:

$$\mu_L^{lt} = 0.001\mu_L, \quad \mu_T^{lt} = 0.001\mu_T, \quad \tau_{fs} = 10 \text{ s}, \quad \tau_d = 10 \text{ s}.$$

The coefficients thermal expansion of the composite material are [24]:

$$\alpha_1 = 0.2(10^{-6})/°\text{C}, \quad \alpha_2 = 28.8(10^{-6})/°\text{C},$$

while the parameters used for the WLF law are [23]:

$$T_{ref} = 143°\text{C}, \quad C_1 = 52, \quad C_2 = 243°\text{C}.$$

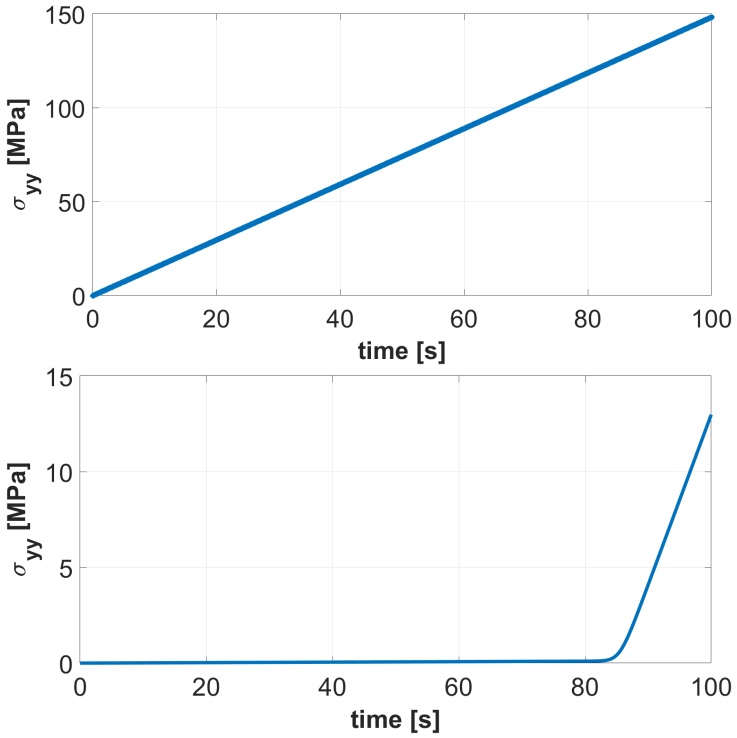

Figure 10: Thermal stresses induced by a linear temperature history when the relaxation is inhibited (top) and where the relaxation is allowed (bottom)

Two different situations were considered. In the first, a null strain has been imposed in the transverse isotropic plane ($\varepsilon_{yy} = 0$ and $\varepsilon_{zz} = 0$). This corresponds to blocking both e_h and e_d: thermal stresses develop due to the condition $e_h = 0$, and they cannot relax through the transverse shear term μ_T as $e_d = 0$. Thermal stress can be directly calculated as:

$$\sigma_{yy} = -\frac{e_h^{th}}{S_H} = -\frac{\alpha_2 \Delta T}{S_H}, \tag{38}$$

that corresponds to the result shown in Fig. (10), top.

In the second scenario, a null strain has been imposed only in the transverse direction ($\varepsilon_{yy} = 0$). Both e_h and e_d are non null, and related to each other through the free ε_{zz} term. The stresses which would develop due to e_h^{th} are therefore relaxed through e_d (see Fig. (10), bottom). In particular,

thermal stress relaxation takes place instantaneously in the first part of the simulation, where the temperature is above the reference temperature, but it appears to stop (in the time frame of the analysis) in the second part of the simulation, when the temperature starts to be lower than the reference temperature and the reduced time becomes far smaller than the relaxation time, inhibiting the viscous term.

The final residual stresses differ by one order of magnitude between the two scenarios. In the first scenario, where stress relaxation is completely inhibited, they reach very high values, which would lead to transverse damage within the composite, but this is not accounted for in the present model.

5.2. Structural simulation: residual stress buildup on a cooled infinite plate

In the present Section, following the work presented in [23], the residual stresses induced in an infinite, unconstrained unidirectional plate undergoing a non-uniform cooling process were assessed using the commercial finite-element software Abaqus. Numerical simulations were performed on a small plate volume (Fig. (11), left). The cooling process occurs through the external surfaces, where an exponential decay temperature function has been imposed. The thermal problem has been solved numerically in Abaqus, setting the following thermal material properties:

$$\rho = 1598 \text{ kg/m}^3, \quad C = 930 \text{ J/(kg K)}, \quad k = 0.4 \text{ W/(m K)},$$

where ρ is the density, C is the specific heat and k is the conductivity.

The temperature history obtained from the thermal computation was used as input to the mechanical problem, in which the material behavior of the composite was defined by an UMAT based on the proposed model. The mechanical boundary conditions are schematically represented in Fig. (11), right. Specifically, the plate volume can deforms in the thickness direction (z-axis), but the two faces of normals x and y are constrained to remain planar, which represents the effect of the infinite surrounding plate. The parameters for the mechanical simulation are the same as in Section 5.1.3.

Residual stresses in the transverse direction were assessed imposing different cooling rates on the external surfaces of the plate volume as depicted in Fig. (12). The outer portions of the plate are the first to reach room temperature, and then act as a constraint to the inner portions, which are not able to contract freely during cooling. A well-known residual stresses profile, with tension at the core and compression close to the surface, develops in the

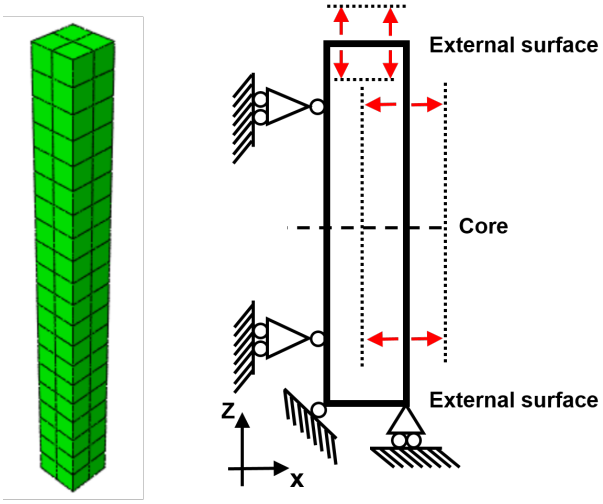

Figure 11: Plate volume simulated in Abaqus (left) and schematic representation its mechanical boundary conditions (right)

plate. As it can be noted, this effects is exacerbated by high cooling rated, which lead to significant through-thickness temperature gradient. On the other hand, it becomes negligible for slow cooling rates, the limit case being a uniform cooling, which would lead to no internal stresses at the ply's scale for a unidirectional composite.

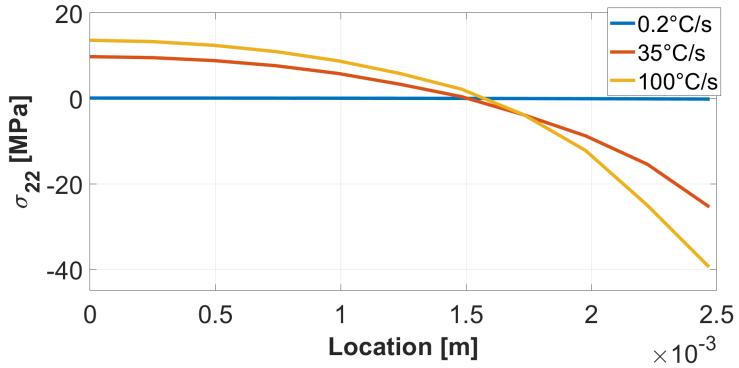

Figure 12: Final residual stress through the thickness in the transverse direction for different initial surfaces cooling rates .

As we have mentioned before, the numerical simulation performed here is inspired by the work presented in [23]. Some differences, however, exist

between the simulations in [23] and the present work. Indeed, [23] includes the crystallization kinetics of the polymeric matrix, which intervenes as an extra source term in the thermal problem, and as an extra source of inelastic deformation in the mechanical problem. On the other hand, the mechanical model is far simpler, involving an incremental elastic description of the stress/strain relation in order to mimic the viscoleastic behavior. For this reason, the results from [23] are similar, but not identical, to those reported here.

6. Conclusions and perspectives

A thermo-viscoelastic constitutive model suited for unidirectional fiber reinforced composite material was presented. In order to highlight the contributions of the fibers and the polymeric matrix, a Cartan decomposition for the stress and the strain tensors was used. The energy function, based on an integrity basis of the decomposition, enabled us to obtain uncoupled constitutive equations in which fibers and matrix contribution are easily recognized. A generalized Maxwell model was applied only to the terms of the decomposition which are affected by the viscoelasticity of the matrix, in agreement with the underlying physical mechanism. The temperature dependence was introduced through the time-temperature superposition principle using the Williams–Landel–Ferry shift function. Thermal strains were included using the same Cartan decomposition.

A first perspective of this work would be to derive the constitutive law for the composite from homogenization of a fiber/matrix representative volume element, and to use the homogenized behavior to identify the material parameters introduced here. This should enable us to validate the choice operated in the paper, that is to consider the viscoelastic contribution only for parameters μ_L and μ_T, and also to identify the respective viscoelastic relaxation functions in terms of the matrix behavior.

As the model was developed in the framework of residual stresses and strain prediction for thermoplastic matrix composites, it will be used in further work to simulate the initial state of LATP manufactured parts. To this aim, it may be necessary to address in the model other physical mechanisms which could affect the development of residual stresses and strains, such as the effect of crystallization of the matrix on the mechanical behavior. The stress/strain decomposition proposed here should make this task relatively easy to achieve.

Acknowledgements

This work was funded by Cetim within the framework of the *Laboratoire Commun Comp'Innov*.

The authors would like to acknowledge Dr. Emmanuel Baranger for developing the Matlab to UMAT conversion tool, which made the UMAT development a matter of hours (instead of days).

References

[1] P.K. Mallick. *Fiber-Reinforced Composites: Materials, Manufacturing, and Design, Third Edition*. Mechanical Engineering. Taylor & Francis, 2008.

[2] I.M. Ward and J. Sweeney. *An Introduction to the Mechanical Properties of Solid Polymers*. Wiley, 2004.

[3] M. Kaliske and H. Rothert. Formulation and implementation of three-dimensional viscoelasticity at small and finite strains. *Computational Mechanics*, 19(3):228–239, 1997.

[4] M. A. Zocher, S. E. Groves, and D. H. Allen. A three-dimensional finite element formulation for thermoviscoelastic orthotropic media. *International Journal for Numerical Methods in Engineering*, 40:2267–2288, 1997.

[5] H. E. Pettermann and A. DeSimone. An anisotropic linear thermo-viscoelastic constitutive law. *Mechanics of Time-Dependent Materials*, 22:4210433, 2018.

[6] M. Kaliske. A formulation of elasticity and viscoelasticity for fibre reinforced material at small and finite strains. *Computer Methods in Applied Mechanics and Engineering*, 185:225–243, 2000.

[7] B. Nedjar. A time dependent model for unidirectional fibre-reinforced composites with viscoelastic matrices. *International Journal of Solids and Structures*, 48:2333–2339, 2011.

[8] A. J. M. Spencer. *Continuum theory of the mechanics of fibre-reinforced composites*, volume 282 of *CISM Courses and Lectures*, chapter Constitutive theory for strongly anisotropic solids. Springer-Verlag Wien GMBH, 1984.

[9] M. Golubitsky, I. Stewart, and D. G. Schaeffer. *Singularities and groups in bifurcation theory. Vol. II*, volume 69 of *Applied Mathematical Sciences*. Springer-Verlag, New York, 1988.

[10] J.-P. Boehler. *Application of tensor functions in solid mechanics*. CISM Courses and Lectures. Springer-Verlag, Wien, 1987.

[11] R.S. Lakes. *Viscoelastic Materials*. Cambridge University Press, 2009.

[12] W. Fulton and J. Harris. *Representation theory*, volume 129 of *Graduate Texts in Mathematics*. Springer-Verlag, New York, 1991. A first course, Readings in Mathematics.

[13] R. Desmorat and R. Marull. Non-quadratic kelvin modes based plasticity criteria for anisotropic materials. *International Journal of Plasticity*, 27, 2011.

[14] R. Desmorat, A. Mattiello, and J. Cormier. A tensorial thermodynamic framework to account for the γ' rafting in nickel-based single crystal superalloys. *International Journal of Plasticity*, 95:43 – 81, 2017.

[15] A. Mattiello, R. Desmorat, and J. Cormier. Rate dependent ductility and damage threshold: Application to nickel-based single crystal cmsx-4. *International Journal of Plasticity*, 10 2018.

[16] A. Bertram and J. Olschewski. Anisotropic creep modelling of the single crystal superalloy srr99. *Computational Materials Science*, 5, 1996.

[17] M. W. Biegler and M. M. Mehrabadi. An energy-based constitutive model for anisotropic solids subject to damage. *Mechanics of Materials*, 19:151–164, 1995.

[18] B. Desmorat, M. Olive, N. Auffray, R. Desmorat, and B. Kolev. Computation of minimal covariants bases for 2d coupled constitutive laws, 2020.

[19] Narindra Ranaivomiarana. *Simultaneous optimization of topology and material anisotropy for aeronautic structures*. PhD thesis, 2019.

[20] R. L. Taylor, K. S. Pister, and G. L. Goudreau. Thermomechanical analysis of viscoelastic solids. *International Journal for Numerical Methods in Engineering*, 2:45–59, 1970.

[21] J. Sorvari and J. Hämäläinen. Time integration in linear viscoelasticity - a comparative study. *Mechanics of Time-Dependent Materials*, 14:307–328, 2010.

[22] *ABAQUS/Standard User's Manual, Version 6.11.* Dassault Systèmes Simulia Corp, United States, 2011.

[23] T. J. Chapman, J. W. Gillespie Jr., R. B. Pipes, J.-A. Manson, and J. C. Seferis. Prediction of process-induced residual stresses in thermoplastic composites. *Journal of Composite Materials*, 24:616–643, 1990.

[24] D. M. Grogan, C. M. Ó Brádaigh, J. P. McGarry, and S. B. Leen. Damage and permeability in tape-laid thermoplastic composite cryogenic tanks. *Composites Part A: Applied Science and Manufacturing*, 78:390–402, 2015.